ROCKET-SPACE DEVICE ENGINEERING AND INFORMATION SYSTEMS
Vol. 7, Iss. 4, 2020, pp. 19–33

Synchronous Addition of Antenna Signals with a Shift of Sampling Pulses in Idealized Mode of Spacecraft Tracking by Target Designations

S.I. Vatutin, *Cand. Sci. (Engineering), Senior Researcher, vatutin.si@spacecorp.ru*
Joint Stock Company "Russian Space Systems", Moscow, Russian Federation

Abstract: The method of synchronous addition of signals of separate antennas was proposed previously for the aggregation of relatively small-scale aperture antennas into a single digital antenna array (digital antenna field) with a combined area for receiving telemetry signals from spacecraft. In this case, the antennas are mutually spaced by a big enough distance in order to not shade one another. The method is based on the idea of compensating the mutual delays between the antennas of the received signal by a corresponding shift of the sampling pulses of the signals of different antennas.
This article demonstrates the method's workability in idealized mode of spacecraft tracking by target designations on orbits of global navigation systems. It is shown that with the up-to-date level of impulse technology development the method of synchronous addition of antenna signals with a shift of sampling pulses is potentially capable of ensuring the reception of telemetry information from deep-space spacecraft at rates approximately 6 times higher than those of the classic Delta-DOR method.

Keywords: antenna array, synchronous addition of signals, intermediate frequency, path difference, propagation delay, target designations, signal-to-noise ratio, bit-error probability

Introduction

Antennas are the main factor in restraining the miniaturization of radio engineering systems and complexes. Everything in the receiver lends itself to miniaturization, except for the antenna, since the energy potential of a radio link is largely determined by its size. However, general digitalization in this area also offers attractive technical solutions for reducing the size of the antennas used by switching from large antennas to digital antenna arrays (DAR) and digital antenna fields. So in radio astronomy, there has been a transition from giant antennas with a diameter of 60–70 m and large antennas with a diameter of 32–34 m to digital antenna fields from antennas with a diameter of about 12 m with synchronous addition of signals from individual antennas in the time domain [1]. Since radio astronomy does not require special efficiency of signal processing, unhurried methods of correlation processing are widely used in VLBI radio interferometers for synchronous addition of radio signals [1, 2]. In this case, the condition of the coherence of the added radio signals, determined by the expression:

$$\Delta T_s \cdot \Delta f << 1, \quad (1)$$

where ΔT_s is the residual time shift between radio signals, Δf is the frequency band of the received radio signal. In VLBI systems, the residual shift ΔT_s is equal to ΔT_d - the sampling period. It is usually considered that "much less than one" is a value of the order of 0.01. However, for different types of modulation, this value can vary over a wide range, both up and down. So, for signals with phase shift keying, it is sufficient that the residual phase shift $\Delta\varphi_o$ does not exceed 0.1 of the phase shift keying value $\Delta\varphi_m$:

$$\Delta\varphi_o \le 0{,}1 \cdot \Delta\varphi_m. \quad (2)$$

With a sampling period ΔT_d, the largest residual phase shift in the signal spectrum will be

$$\Delta\varphi_o = 2\pi \cdot \Delta T_d \cdot \Delta f. \quad (3)$$

Hence, for BPSK with $\Delta\varphi_m = \pi$, we obtain the coherence condition $\Delta T_d \cdot \Delta f \le 0.05$; for QPSK with $\Delta\varphi_m = \pi/2$ we obtain $\Delta T_d \cdot \Delta f \le 0.025$; for 8PSK with $\Delta\varphi_m$ $\pi/4$, we obtain the coherence condition of the added signals $\Delta T_d \cdot \Delta f \le 0.0125$. For higher-order phase-shift keying radio signals, the coherence condition will be more stringent than (1). In any case, the condition for the coherence of radio signals imposes much stricter restrictions on the permissible sampling period of a radio signal than the Kotelnikov (Nyquist) theorem for a radio signal, according to which the condition must be met:

$$\Delta T_d \cdot \Delta f \le 1. \quad (4)$$

Therefore, in radio systems associated with the transmission of information in satellite communications [3], in radar [4-6], in cellular communications [7, 8], in navigation [9, 10], the most widespread are DARs with the traditional addition of information signals in spectral region, when the elementary antennas of the array are located close enough to each other, so that for the time of propagation along the array Δt_p and the bandwidth of the useful signal Δf, the condition of the narrow band of the system is met, that is:

$$\Delta t_p \cdot \Delta f << 1. \quad (5)$$

However, in spacecraft control systems, when constructing the antenna field, on the condition that there is no shadowing of each other within the seven-degree radio visibility zone, the antennas should be separated by at least 8 antenna diameters, that is, by tens of meters. For example, antennas with a diameter of 5 m should be 40 m apart. Therefore, when transmitting telemetry information (TMI) at a speed of 0.5 Mbit/s, harmonics at the edges of the spectrum, spaced approximately at Δf = 1 MHz, will give an unacceptably large phase incursion $\Delta\varphi = 2\pi \cdot \Delta f \cdot \Delta t = 2\pi \cdot \Delta f \cdot (\Delta L/c) = 2\pi \cdot 10^6 \cdot 40/(3 \cdot 10^8)$ = 0,27π.

Thus, in the digital fields of spacecraft tracking, it is not possible to add the signals of the DAR antennas in the spectral region. There remains an attempt to add signals in the time domain, relying on extensive experience in working with VLBI systems. But in these systems, the payoff for the ability to coherently add signals from widely separated antennas is a significant decrease in ΔT_d $\cdot \Delta f$, that is, the information content of the system, which is extremely undesirable for systems for transmitting TMI from spacecraft. Fortunately, here the antennas are not spaced as far apart as in VLBI systems, which allows synchronizing the heterodyne oscillators of the high-frequency cascades of receiving radio signals

from different antennas of the digital antenna field and shifting the sampling pulse grids of signals from different antennas so that samples are taken for the same received radio signal from different antennas on the same front. For this, the sampling period of the radio signal ΔT_d, for which condition (4) is satisfied, must be divided into sufficiently small intervals of the sampling pulse shift ΔT_c, such that they satisfy the coherence condition (1) for the corresponding type of modulation. After that, the sampling pulses of signals from different antennas must be shifted by the corresponding number of shift intervals ΔT_s so that the samples of realizations of the same signal received by different antennas are taken on the same front with an accuracy of ΔT_s. The idea of the method is presented in [11], where a device for synchronous addition of signals with a shift in sampling pulses is proposed. The proposed antenna phasing device is described in detail in the patent [12].

The essence of the method of synchronous addition of radio signals of antennas of a digital antenna field with a shift of sampling pulses

Fig. 1 shows the simplest configuration of the antenna field of three antennas A0, A1, A2, connected by feeders Φ0, Φ1, Φ2 with a synchronous addition device (SAD) of antenna signals, which includes a pulse generator for sampling antenna signals. In fig. 2 is a timing diagram of the sampling for the same edge of the signal received by the antennas. Antenna A0 is a reference antenna; the front of the radio signal wave falls earlier on antenna A1, and later on antenna A2, than on antenna A0.

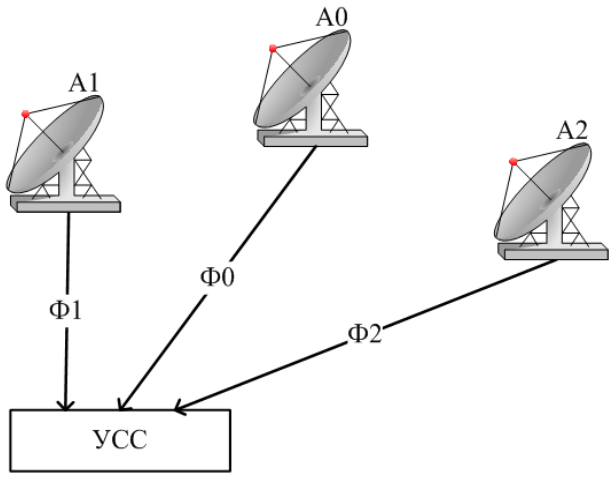

Fig. 1. Simplest antenna field configuration to illustrate the method of synchronous addition of antenna signals

For synchronous addition of the antenna signals, the next k-th sampling pulse of the generator for the information signal of antenna No. i, formed at time t_{Gk}, is delayed for a time

$$\Delta t_{zik} = \Delta t_{ci0k} + \Delta t_{\phi i} - \Delta t_{\phi 0} + \Delta t_p. \quad (6)$$

Here Δt_{ci0k} is the time of the shift of the moment of arrival of the front of the wave of the received signal on the antenna No. i relative to the reference antenna No. 0. It can be negative if the signal arrives at antenna No. i earlier than at antenna No. 0, and positive if the signal arrives at antenna No. i later than antenna No. 0, and changes during the spacecraft›s coverage area. The rest of the delay time terms are constants. So, $\Delta t_{\phi i}$ is the propagation time of the signal wave front in the feeder from the phase center of the antenna No. i to the SAD. To ensure that the sample of the desired front is taken after its arrival at the SAD from all field antennas, an additional delay of the sampling pulse is introduced for the dwell time Δt_p, which is chosen so that the time instant of the k-th sampling pulse on all antennas comes later than the k-th sampling pulse of the generator, that is, from the condition $\Delta t_{zik} > 0$. This condition is always satisfied if the dwell time Δt_p is chosen from the condition

$$\Delta t_p > \Delta t_{\phi max} - \Delta t_{\phi min} + \Delta t_{pmax} + \Delta t_{ADC}, \quad (7)$$

where $\Delta t_{\phi max}$ and $\Delta t_{\phi min}$ are the maximum and minimum propagation times of the signal wave front in the antenna array feeders, respectively, Δt_{pmax} is the maximum possible propagation time of the signal wave front in free space along the cross section of the antenna array, Δt_{ADC} is the ADC count formation time. As the spacecraft moves in the radio visibility zone, there is a change in the magnitude Δt_{ci0k} of the moment shift ΔT_{CI0K} of the arrival of the wave front of the received signal on antenna No. i relative to the reference antenna No. 0, which must be tracked.

It is shown in [13] that when operating with a spacecraft in a reference orbit with an altitude of 200 km, the delay update interval dT_{du} = 0.1 s provides an almost ideal synchronous summation of signals from the antennas of the digital antenna field. However, these assessments were carried out without taking into account the dynamics of the spacecraft tracking system.

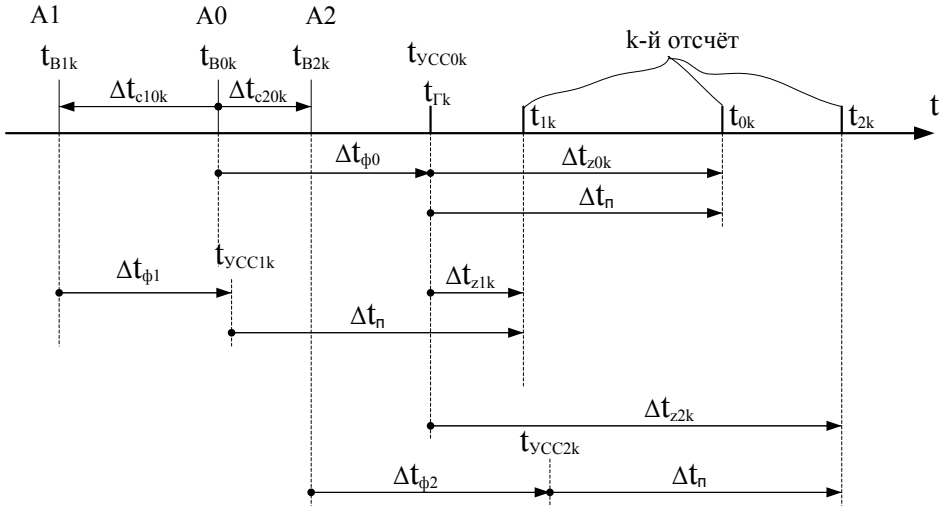

Table 1. Coordinates and lengths of antenna feeders of the considered antenna field

Antenna no.	X	Y	Z	Feeder length
0	0	0	0	60
1	$8 \cdot D_A = 24$	0	0	84
2	$8 \cdot D_A \cdot \cos(1 \cdot 60°) = 12$	$8 \cdot D_A \cdot \sin(1 \cdot 60°) = 20.78$	0	92.78
3	$8 \cdot D_A \cdot \cos(2 \cdot 60°) = -12$	$8 \cdot D_A \cdot \sin(2 \cdot 60°) = 20.78$	0	68.78
4	$8 \cdot D_A \cdot \cos(3 \cdot 60°) = -24$	$8 \cdot D_A \cdot \sin(3 \cdot 60°) = 0$	0	36
5	$8 \cdot D_A \cdot \cos(4 \cdot 60°) = -12$	$8 \cdot D_A \cdot \sin(4 \cdot 60°) = -20.78$	0	68.78
6	$8 \cdot D_A \cdot \cos(5 \cdot 60°) = 12$	$8 \cdot D_A \cdot \sin(5 \cdot 60°) = -20.78$	0	92.78

This work is devoted to testing the fundamental possibility of synchronous addition of antenna signals in the mode of tracking a spacecraft by target designation. As an example, the antenna field of parabolic antennas with a diameter of $D_A = 3$ m was considered in the form of a regular hexagon, inscribed from the condition of non-shadowing over a seven-degree radio visibility zone in a circle with a radius of $8 \cdot D_A = 24$ m with a reference antenna in the center, as shown in Fig. 3. The coordinates of the seven antennas numbered from 0 to 6 and the lengths of the respective feeders are shown in Table 1.

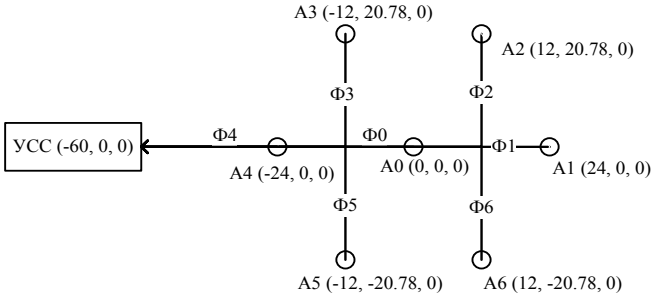

Fig. 3. Antenna field configuration under consideration

Feeder delays are calculated in the model using the obvious formula:

$$\Delta t_{\phi i} = L_{\phi i} \cdot \varepsilon^{1/2}/C, \quad (8)$$

where C is the speed of light in free space, e = 2.2 is the dielectric constant of polyethylene taken as the dielectric of the feeder cable. The residual adjustment error of the delay in the feeder, which affects the accuracy of the addition of antenna signals, in the auto-tracking model is calculated by the formula:

$$\Delta T_{ji} = \Delta T_{jmax} (\text{rand}(1,1) - 0{,}5), \quad (9)$$

where rand (1,1) is a MATLAB random number generator function with uniform distribution on the interval (0, 1), ΔT_{jmax} is the maximum spread in the adjustment of the propagation time in the feeder. During the simulation, it was found that the spread ΔT_{jmax} should not exceed a value commensurate with the permissible interval of the shift of sampling pulses ΔT_s.

Antenna angular motion model

The dynamics of the direction change on the spacecraft is determined by the design of the antenna's rotary support and the parameters of the spacecraft orbit. For azimuth-elevation support-rotary devices, the most dynamic are the near-zenith parts of the spacecraft's low orbits. To assess the dynamic characteristics of tracking, it is sufficient to use the simplest model of the circular motion of the spacecraft at different heights without taking into account the angular motion of the Earth, described in [13]. According to this model, the dependences of the elevation angle Φ(t), azimuth Ψ(t) and the distance to the spacecraft $R_{SC}(t)$ at the time from the moment the spacecraft passes the ascending node are determined by the expressions:

$$\Phi(t) = \arcsin \frac{\sin(\omega_{sc}t) \cdot \cos i - \frac{R}{R+H}}{\sqrt{[\cos(\omega_{sc}t)]^2 + [\sin(\omega_{sc}t) \cdot \sin i]^2 + \left[\sin(\omega_{sc}t) \cdot \cos i - \frac{R}{R+H}\right]^2}}, \quad (10)$$

$$\Psi(t) = \arcsin \frac{\cos(\omega_{sc}t)}{\sqrt{[\cos(\omega_{sc}t)]^2 + [\sin(\omega_{sc}t) \cdot \sin i]^2}}. \quad (11)$$

Distance to SC:

$$R_{sc}(t) = \sqrt{[(R + H)\cos(\omega_{sc}t)]^2 + [(R + H) \cdot \sin(\omega_{sc}t) \cdot \sin i]^2 + [(R + H) \cdot \sin(\omega_{sc}t) \cdot \cos i - R]^2},$$

here ω_{SC} is the angular velocity of the spacecraft in the orbital plane,

$$\omega_{SC} = \frac{R}{R+H}\sqrt{\frac{g}{R+H}} = \frac{v_{1sc}}{R+H}\sqrt{\frac{R}{R+H}}, \quad (12)$$

where R = 6371 km is the mean radius of the Earth, g = 9.8 is the acceleration of gravity on the Earth's surface, v_{1SC} = 7.93 km/s– is the first space velocity, H is the height of the spacecraft orbit, *i* is the angle between the spacecraft orbit plane and direction to the zenith of the observer, α is the angle in the orbital plane between the direction to the ascending node and the current direction to the spacecraft at time t. The angle α_0 of the beginning of the RVZ is determined by the expression:

$$\alpha_0 = \arcsin \frac{R}{(R+H)\cos i}. \quad (13)$$

The start time t_{sz}, the end t_{ez} of the radio visibility zone and the time at the parameter t_p at the highest point of the orbit for the observer is determined by the obvious expressions:

$$t_{sz} = \frac{\alpha_0}{\omega_{SC}}, \; t_{ez} = \frac{\pi - \alpha_0}{\omega_{SC}}, \; t_p = \frac{\pi}{2\omega_{SC}}. \quad (14)$$

From (11) it follows that the maximum absolute angular azimuthal velocity of the spacecraft on the parameter is determined by a simple relation:

$$\Psi'_p \approx \frac{-\omega_{sc}}{\sin i} \quad (15)$$

From (15) we see: the closer the orbit is to the zenith, the higher the azimuthal angular velocity of the spacecraft in the near-zenith zone. Currently, triaxial antennas are used to work directly in the zenith zone, which, however, have a limited maximum bank angle from 10° to 14° for different manufacturers. Accordingly, up to an angle of 76°–80°, these three-axis antennas operate in the biaxial azimuth-elevation mode. Therefore, in this work, all assessments were carried out based on the most unfavorable angle for the azimuth-elevation regime at a parameter of 80°.

Information signal model

At the time t at the intermediate frequency f_p, the model assumes the reception of a quadrature phase-shift keyed signal of the form

$$U(t) = U_c(t) \cdot [\cos(2 \cdot \pi \cdot f_p \cdot t + \varphi + \psi(t)) + j \cdot \sin(2 \cdot \pi \cdot f_p \cdot t + \varphi + \psi(t))] \quad (16)$$

where $U_c(t)$ is the signal amplitude at time t, φ = π/4 is the constant phase of the signal, ψ(t) is the changing (manipulated) phase of the signal with the manipulation frequency F_m. We will make estimates for a BPSK signal of the meander type, in which the phase keying is carried out according to the law:

$$\psi(t) = sign(\cos(2 \cdot \pi \cdot F_m \cdot t)) \cdot (\pi/2). \quad (17)$$

The power of the signal S received from the spacecraft through the diameter of a single parabolic receiving antenna is determined by the well-known formula:

$$P_{r1}(t) = \frac{P_t \cdot G_t \cdot \eta_p \cdot K_{ef} \pi \cdot D_A^2}{16 \cdot (R_{sc}(t))^2}, \quad (18)$$

where the parameters used in the model have the following values: $\eta_p = \eta_t \cdot \eta_r \cdot \eta_{pol} \cdot \eta_n$ is the resulting coefficient of losses when transmitting the signal, P_t=10 W is the power of the transmitter, G_t=2 is the transmitter antenna gain, η_t=0.78 is the transmitter AFS efficiency, η_r= 0.78 is the receiver AFC efficiency , η_{pol}= 0.69 is the polarization loss coefficient, η_n = 0.95 is the loss factor from inaccurate antenna pointing, K_{ef} = 0.5 is the antenna efficiency factor. Amplitude of the signal S received by a single antenna:

$$U_{S1} = \sqrt{2R_A P_{r1}}, \quad (19)$$

where R_A = 75 Ohm is the equivalent antenna impedance.

The level of the signal received from the spacecraft depends on the angle of deflection of the antenna from the direction to the spacecraft. If the signal amplitude of a single antenna with the exact direction of its diagram on the spacecraft is equal to U_{S1} then when its diagram deviates by an angle Θ, the signal amplitude will be equal to

$$U_{S1\Theta} = U_{S1} \cdot F(\Theta), \quad (20)$$

where F (Θ) is the normalized radiation pattern of a single parabolic antenna, which for estimation calculations is approximated by the known expression [16]:

$$F(\Theta) = \exp[-a \cdot (\Theta/\Theta_{0,5})^2]. \quad (21)$$

Here $\Theta_{0.5}$ is half of the radiation pattern width at the level of 0.5 signal power and at the level of 0.707 of the signal amplitude, with a = 0.346574.

It is known [16] that the width of the directional pattern of an antenna with a diameter D at the level of 0.5 signal power at a carrier with a wavelength λ is determined by the expressions:

$$\Delta\Theta_{0,5} = 1{,}12 \cdot \lambda/D, \text{ rad},$$
$$\Delta\Theta_{0,5} = 64 \cdot \lambda/D, \text{ degrees} \quad (22)$$

It is assumed here that the transmission of TMI from the spacecraft is carried out in the D4 range on the carrier f_n = 2.3 GHz, while the wavelength λ = 13 cm, and the width of the directional pattern of a three-meter antenna is 2.78 °. With a simultaneous deviation from the direction to the spacecraft in elevation by ΔΨ and in azimuth by an angle ΔΦ, we have:

$$\Phi_{RP} = \Phi_{SC} + \Delta\Phi, \Psi_{RP} = \Psi_{SC} + \Delta\Psi, \quad (23)$$

moreover, the resulting deflection angle at the j-th tracking step Θ_j = arccos ($\cos\Theta_j$) is obtained from the ratio for the angle between the directional pattern vector and the directional vector to the spacecraft through the corresponding direction cosines of the antenna pattern and spacecraft:

$$\cos\Theta_j = \cos\alpha_{RPj-1} \cdot \cos\alpha_{SCj} + \\ + \cos\beta_{RPj-1} \cdot \cos\beta_{SCj} + \cos\gamma_{RPj-1} \cdot \cos\gamma_{SCj}. \quad (24)$$

It is assumed here that the duration of the tracking (simulation) step is dT = ($t_j - t_{j-1}$) = 0.1 s. The direction cosines of the antenna array antenna patterns and the direction to the spacecraft at the j-th tracking step in the local (topocentric) coordinate system are determined by the known formulas through the azimuth and elevation angle of the radiation pattern and direction to the spacecraft, respectively:

$$\cos(\alpha_{RPj}) = \cos(\Phi_{RPj}) \cdot \sin(\Psi_{RPj}),$$
$$\cos(\alpha_{SCj}) = \cos(\Phi(t_j)) \cdot \sin(\Psi(t_j)), \quad (25)$$

$$\cos(\beta_{RPj}) = \cos(\Phi_{RPj}) \cdot \cos(\Psi_{RPj}),$$
$$\cos(\beta_{SCj}) = \cos(\Phi(t_j)) \cdot \cos(\Psi(t_j)), \quad (26)$$

$$\cos(\gamma_{RPj}) = \sin(\Phi_{RPj}),$$
$$\cos(\gamma_{SCj}) = \sin(\Phi(t_j)). \quad (27)$$

The difference in the path of the beams from the direction of the antenna pattern at the (j – 1)-th step of tracking between antennas No. i (A_i) and the reference antenna No. 0 (A_0) is determined by the formula:

$$\Delta R_{i0RPj-1} = L_{i0} \cdot \cos(<A_i - 0 - RP_{j-1}) = \\ = L_{i0} \cdot [\cos(\alpha_{i0}) \cdot \cos(\alpha_{RPj-1}) + \cos(\beta_{i0}) \cdot \cos(\beta_{RPj-1}) + \\ + \cos(\gamma_{i0}) \cdot \cos(\gamma_{RPj-1})]. \quad (28)$$

Here L_{i0} is the distance between the phase centers of the antennas A_i and A_0, $\cos(\alpha_{i0})$, $\cos(\beta_{i0})$, $\cos(\gamma_{i0})$ are the direction cosines of the vectors from the reference antenna A_0 to the antenna A_i, calculated by the formulas:

$$L_{i0} = \sqrt{(x_i - x_0)^2 + (y_i - y_0)^2 + (z_i - z_0)^2}, \quad (29)$$

$$\cos(\alpha_{i0}) = (x_i - x_0)/L_{i0},$$
$$\cos(\beta_{i0}) = (y_i - y_0)/L_{i0}, \quad (30)$$
$$\cos(\gamma_{i0}) = (z_i - z_0)/L_{i0},$$

where (x_i, y_i, z_i) and (x_0, y_0, z_0) are the coordinates of the phase centers of the antennas A_i and A_0 in the local coordinate system.

The shift in time of arrival of the radio signal between the antennas A_i and A_0 from the direction of aiming the radiation pattern $\Delta t_{ci0RPj-1}$ is used in the device for synchronous addition of antenna signals throughout the entire j-th tracking step and is determined by the formula

$$\Delta t_{ci0RPj-1} = \Delta R_{i0RPj-1}/C, \quad (31)$$

where C is the speed of light in free space.

The difference between the path of the beams from the direction to the spacecraft at the j-th tracking step between antennas No. i (A_i) and the reference antenna No. 0 (A_0) is determined by the formula

$$\Delta R_{i0SCj} = L_{i0}\cdot\cos(<A_i–0–SCj)= \\ = L_{i0}\cdot[\cos(\alpha_{i0})\cdot\cos(\alpha SC_j) + \cos(\beta_{i0})\cdot\cos(\beta SC_j) + \\ + \cos(\gamma_{i0})\cdot\cos(\gamma SC_j)]. \quad (32)$$

Accordingly, we obtain a shift in time of arrival of the radio signal between antennas A_i and A_0 from the direction to the spacecraft:

$$\Delta t_{ci0SCj} = \Delta R_{i0SCj}/C. \quad (33)$$

Taking into account the time rounding in the SAD by the value of the unit interval of the sampling pulse shift ΔT_s and the adjustment error ΔT_{ji} of the signal propagation time from the antenna A_i along the feeder line to the SAD, we obtain the following estimate of the shift incursion in the time of arrival of the radio signal between the antennas A_i and A_0 for the j-th tracking step T_0 from t_{j-1} to t_j:

$$\Delta t_{ci0j} = \text{round}(\Delta t_{ci0RPj-1}/\Delta T_c)\cdot\Delta T_s - \Delta t_{ci0SCj} + \Delta T_{ji}. \quad (34)$$

The sine component of the clean information signal of the i-th antenna at the j-th step:

$$UI_{Sij} = U_{S1j}\cdot F(\Theta_j)\cdot\sin(2\pi F_{IF}\cdot t_j + \pi/4 - 2\pi F_{IF}\cdot\Delta t_{ci0j} + \\ + \text{sign}(\cos(2\pi F_{MH}\cdot t_j - 2\pi F_{MH}\cdot\Delta t_{ci0j}))\cdot\pi/2). \quad (35)$$

The cosine component of the clean information signal of the i-th antenna at the j-th step:

$$UI_{Cij} = U_{S1j}\cdot F(\Theta_j)\cdot\cos(2\pi F_{IF}\cdot t_j + \pi/4 - 2\pi F_{IF}\cdot\Delta t_{ci0j} + \\ + \text{sign}(\cos(2\pi F_{MH}\cdot t_j - 2\pi F_{MH}\cdot\Delta t_{ci0j}))\cdot\pi/2). \quad (36)$$

Single antenna noise power:

$$P_{N1}=2\cdot k_0\cdot t^\circ\cdot m_{sl}\cdot R_i, \quad (37)$$

where $k_0 = 1.38\cdot10^{-23}$ is the Boltzmann constant, t° = 200° K is the equivalent noise temperature of the receiver input stage, R_i is the information transfer rate, m_{sl} = 1.25 is the number of radio signal spectrum lobes.

It should be noted that in the developed model of spacecraft tracking, the sampling frequency F_d of the signal at the intermediate frequency F_{IF} is selected based on the condition of minimum distortions due to overlaps of the spectra of the original radio signal multiplied during sampling with an estimate of the upper frequency $F_w = m_{ls}\cdot R_i$ in accordance with the formula [15, 16]

$$F_d = \frac{4F_{IF}}{2m_d + 1}, \quad (38)$$

where the discretization order m_d is chosen, in turn, by the formula

$$m_d = \text{floor}\left(\frac{F_{IF} - F_B}{2F_B}\right) \quad (39)$$

Noise power of a single sampling channel (sine or cosine):

$$P_{n1d} = P_{n1}/2. \quad (40)$$

Single antenna root-mean-square noise deviation:

$$\sigma_{n1} = \sqrt{2R_A P_{n1}}. \quad (41)$$

RMS noise deviation for a single sampling channel (sine or cosine):

$$\sigma_{n1d} = \sqrt{R_A P_{n1}}.$$

Signal-to-noise power ratio for a single antenna:

$$SNR_1 = \frac{P_{r1}}{P_{n1}} \quad (42).$$

Signal-to-noise power ratio with absolutely synchronous addition of signals from all antenna arrays:

$$SNR_{ALL} = \frac{(N_A U_{S1})^2}{(2\cdot R_A)\cdot(N_A\cdot P_{n1})} = \frac{N_A P_{r1}}{P_{n1}}. \quad (43)$$

The noise value in the sine and cosine information channel of sampling of the i-th antenna at the j-th tracking step is calculated using different samples of the MATLAB randomization function for the normal distribution law:

$$U_{ISnij} = \sigma_{n1d}\cdot\text{randn}(1,1),\ U_{ICnij} = \\ = \sigma_{n1d}\cdot\text{randn}(1,1). \quad (44)$$

The sine component of the noisy information signal of the i-th antenna:

$$UI_{c+nSij} = UI_{Sij} + U_{ISnij}. \quad (45)$$

The cosine component of the noisy information signal of the i-th antenna:

$$UI_{c+nCij} = UI_{Cij} + U_{ICnij}. \quad (46)$$

Amplitude of the net total information signal of all antennas of the field:

$$UI_j = \sqrt{\left(\sum_{i=0}^{N} UI_{Cij}\right)^2 + \left(\sum_{i=0}^{N} UI_{Sij}\right)^2} \quad (47)$$

Amplitude of the net total information signal of all antennas of the field:

$$UI_{s+nj} = \sqrt{\left(\sum_{i=0}^{N} UI_{s+nCij}\right)^2 + \left(\sum_{i=0}^{N} UI_{s+nSij}\right)^2} \quad (48)$$

Amplitude of the net total information signal of all antennas of the field:

$$\varphi_j = \text{sign}\left(\sum_{i=0}^{N} UI_{s+nSij}\right) \cdot \text{acos}\left(\frac{\sum_{i=0}^{N} UI_{c+nCij}}{UI_{s+nj}}\right). \quad (49)$$

In practice, the signal-to-noise ratio cannot be determined in practice, since, in accordance with (49), at the reception we always deal with a mixture of signal and noise, from which it is impossible to isolate a pure signal [17]. However, the model contains estimates of the amplitude of both the pure signal of a single antenna (19) and the pure total signal of all antennas of the field (48), taking into account the tracking errors. Hence the signal-to-noise ratio with ideal addition of antenna signals without taking into account tracking errors:

$$SNR_{Idj} = \frac{(N+1)\cdot U_{S1j}{}^2}{2\cdot R_A\cdot(N+1)\cdot P_{N1}} = \frac{U_{S1j}{}^2}{2\cdot R_A\cdot P_{N1}}. \quad (50)$$

Real signal-to-noise ratio including tracking errors:

$$SNR_{Rej} = \frac{UI_j{}^2}{2\cdot R_A\cdot(N+1)\cdot P_{N1}}. \quad (51)$$

Finally, the probability of a bit error according to Kotelnikov V.A. [19]:

$$P_{ONBj} = \frac{1}{2} - \text{erf}\left(\sqrt{SNR_{Rej}\cdot\frac{1-\rho}{2}}\right)/2, \quad (52)$$

where $\rho = -1$ is the correlation coefficient for phase shift keying by π.

Simulation results

To calculate the delays, it is necessary to interpolate the values of the elevation and azimuth in the intervals between the nodal moments of target designations (TD). If n_{TD} is the number of simulation (tracking) steps dT in the target designation period dT_{TD}, then with linear interpolation, the calculated elevation angles Φ_{RPj+1p} and azimuth Ψ_{RPj+1p} on the (j + 1)-th step of tracking will be determined by the expressions:

$$\Phi_{RPj+1p} = \Phi_{SC}(t_{(floor(j/n_{TD})\cdot n_{TD+1})}) + \\ + (\Phi_{SC}(t_{(ceil(j/n_{TD})\cdot n_{TD+1})}) - \\ - \Phi_{SC}(t_{(floor(j/n_{TD})\cdot n_{TD+1})}))/n_{TD}\cdot(j - floor(j/n_{TD})),$$

$$\Psi_{RPj+1p} = \Psi_{SC}(t_{(floor(j/n_{TD})\cdot n_{TD+1})}) + \\ + (\Psi_{SC}(t_{(ceil(j/n_{TD})\cdot n_{TD+1})}) - \\ - \Psi_{SC}(t_{(floor(j/n_{TD})\cdot n_{TD+1})}))/n_{TD}\cdot(j - floor(j/n_{TD})). \quad (53)$$

Modeling confirmed the results of [13] that in a reference orbit with an altitude of 200 km, it is desirable to keep the update period of delays dT_{du} in the digital antenna field at a level of 0.1 s, but at the same time showed that in low orbits it is advisable to work with single antennas with a diameter about 3 m, and they should be combined into a single antenna field with the addition of signals to increase the energy potential of the radio link when working with a high-orbit spacecraft.

As shown in fig. 4, during the transition from low orbits with an altitude of 200 km (Fig. 4, *a*, *b*) to high orbits with an altitude of 20,000 km (Fig. 4, *c*, *d*), the dynamics of changes in elevation angles, azimuth significantly decreases (Fig. 4, *a*, *c*) and the delays of the radio signal between the antennas (Fig. 4, *b*, *d*), which makes it possible to painlessly increase the periods of target designations and update delays in digital antenna fields.

Fig. 5 illustrates the idealized spacecraft tracking mode in an orbit with an altitude of 20,000 km, which is typical for global navigation systems. Based on the parameters of the system for the reference orbit (dT_{TD} = 1 s; dT_{du} = 0.1 s), we select the period of the TD dT_{TD} and the update period of the delays dT_{du} for the high orbit at an intermediate frequency F_{if} = 70 MHz at the clock frequency of the sampling pulses shift $F_s = 1/\Delta T_s$ = 2 GHz. For the initial parameters, the diagram of the BP deviation towards the spacecraft is shown in Fig. 5, *a*, the modulus of the signal amplitude in Fig. 5*b*, the signal-to-noise ratio in Fig. 5*c* and the probability of a bit error in Fig. 5, *d* from 10^{-4} at the edges of the RVZ to 10^{-6} for the elevation angle on the parameter at the TMI transmission rate R = 256 Kbit/s.

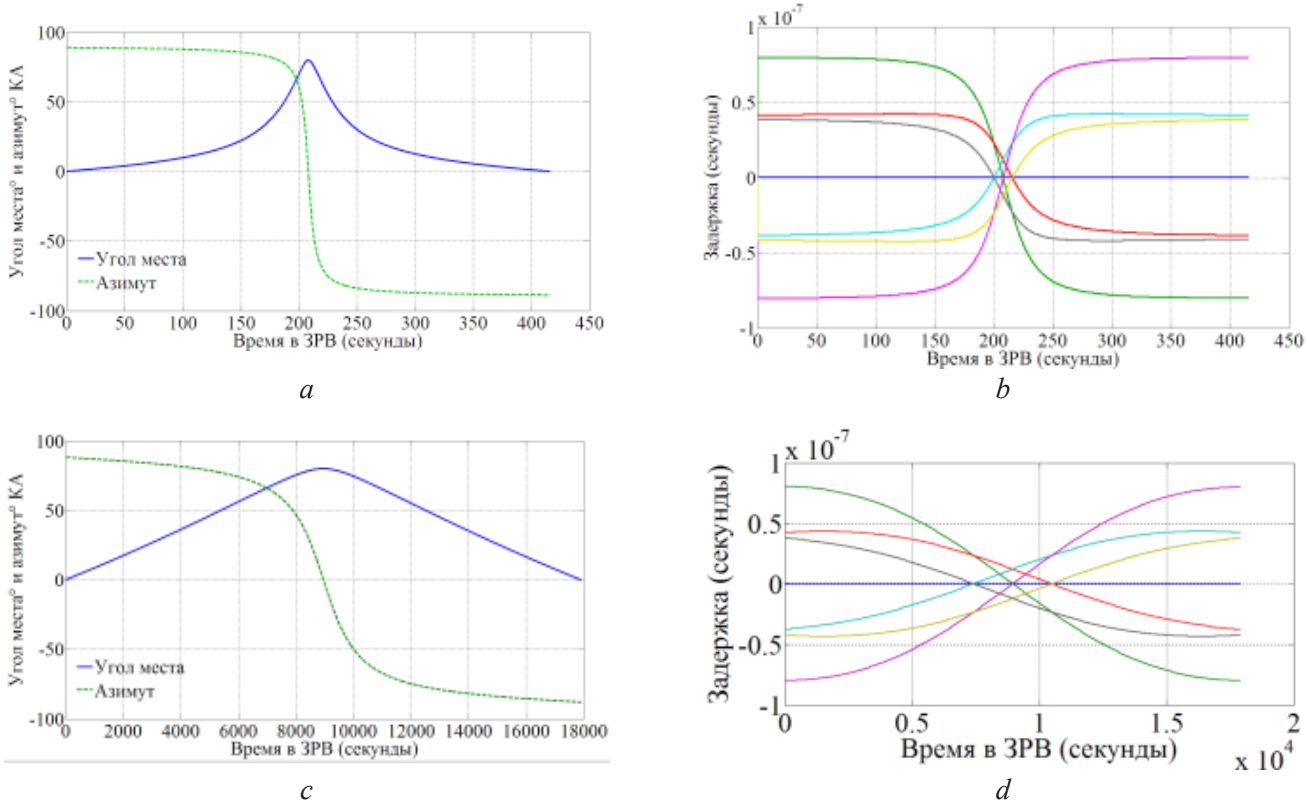

Fig. 4. Reducing the dynamics of changes in elevation angles, azimuth and delays during the transition from low to high spacecraft orbits

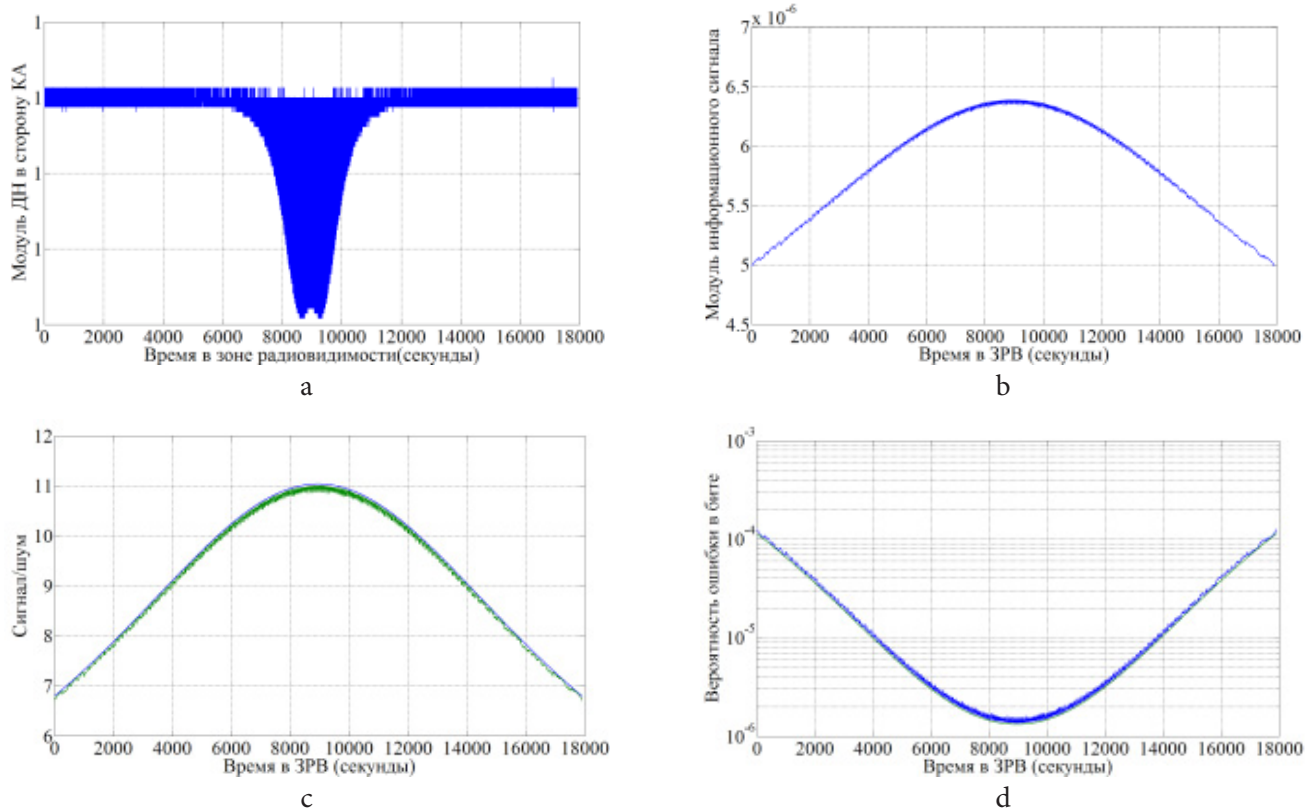

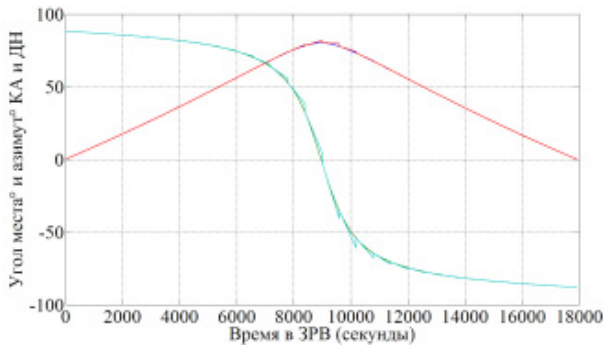
Угол места° и азимут° КА и ДН
Время в ЗРВ (секунды)

e

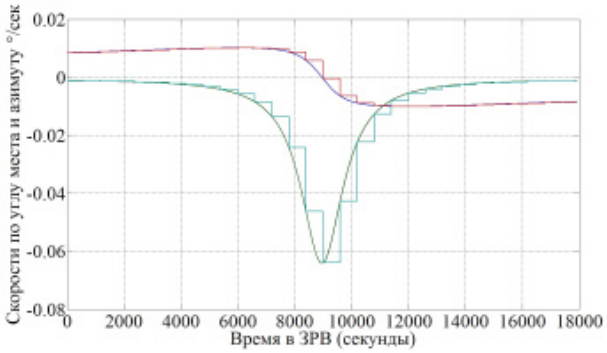
Скорости по углу места и азимуту °/сек
Время в ЗРВ (секунды)

f

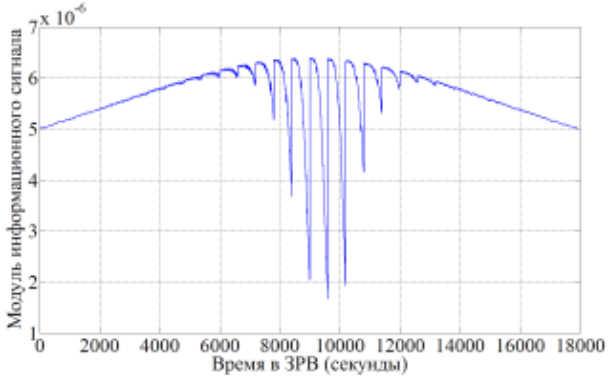
x 10^-6
Модуль информационного сигнала
Время в ЗРВ (секунды)

g

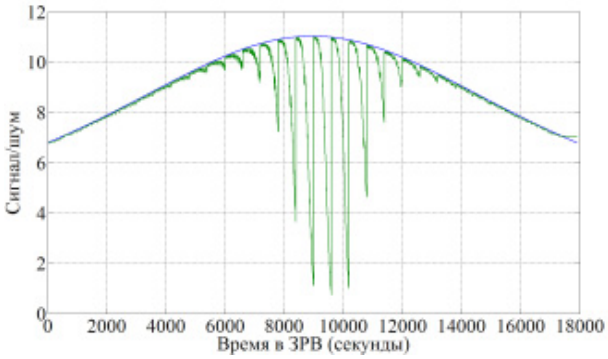
Сигнал/шум
Время в ЗРВ (секунды)

h

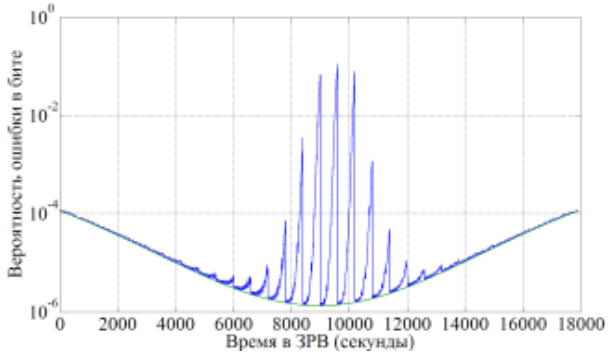
Вероятность ошибки в бите
Время в ЗРВ (секунды)

i

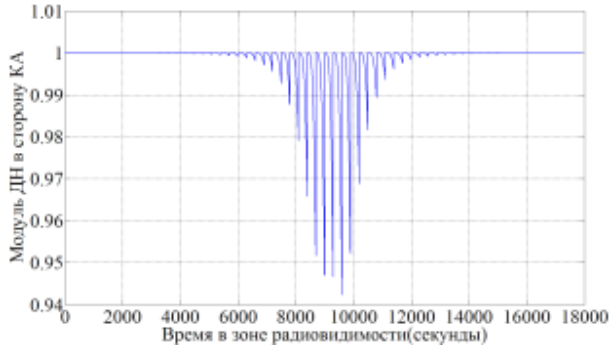
Модуль ДН в сторону КА
Время в зоне радиовидимости(секунды)

j

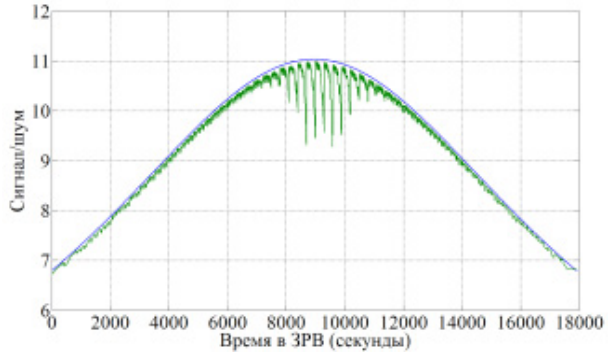
Сигнал/шум
Время в ЗРВ (секунды)

k

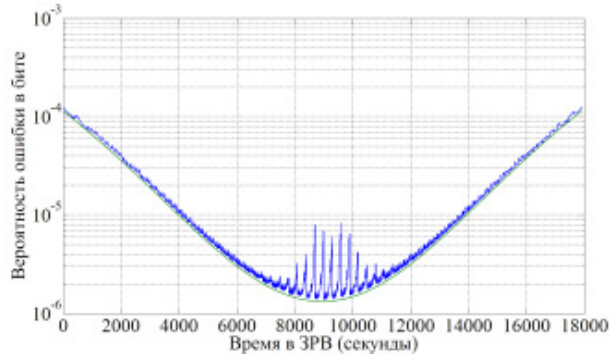
Вероятность ошибки в бите
Время в ЗРВ (секунды)

l

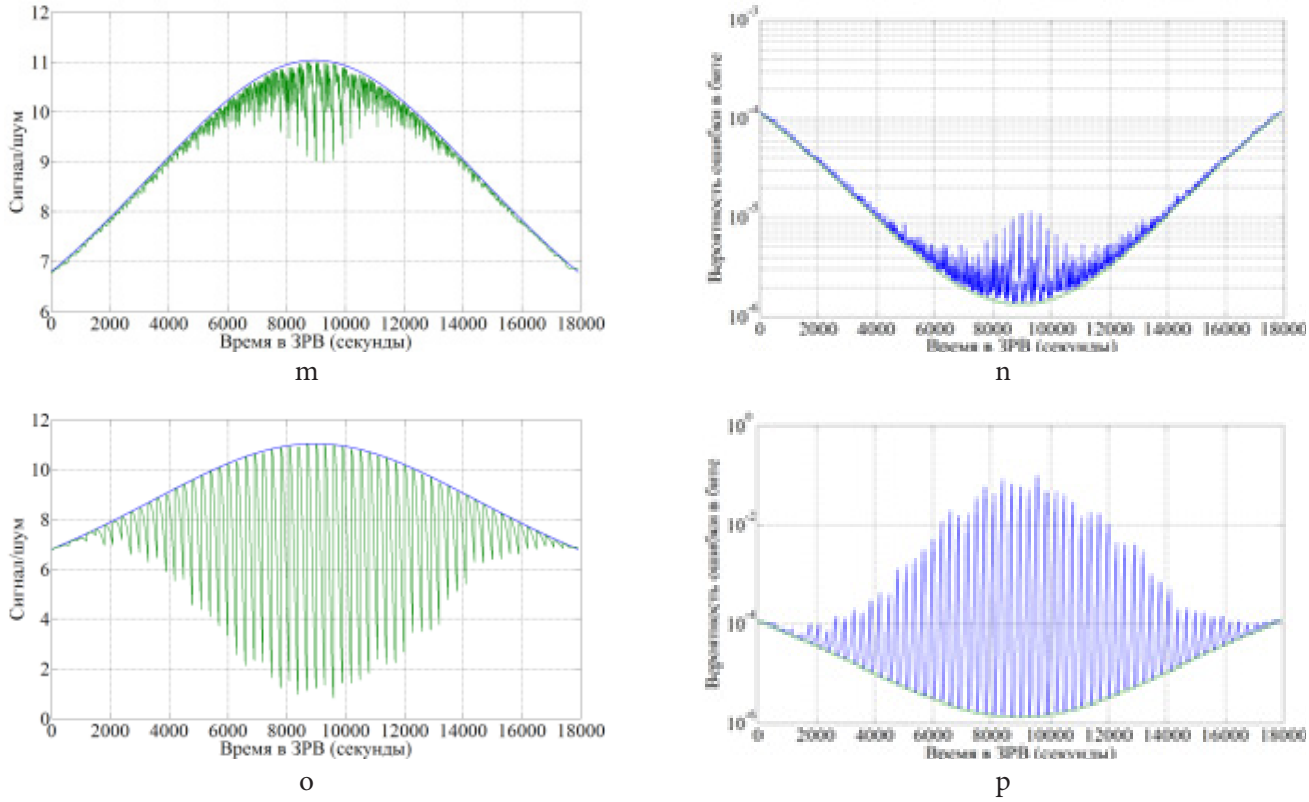

Fig. 5. Selection of TD interval and delay update interval

It is obvious that the initial dT_{TD} and dT_{du} are too small. An increase in the CS interval to 10 min lowers the minimum of the RP towards the spacecraft to 0.4, makes the jumps in angles (Fig. 5, *e*) and velocities (Fig. 5, f) noticeable.

At the nodal points of the TD, on the dynamic segment of the spacecraft trajectory, the signal falls below the values at the edges of the RVZ (Fig. 5, *g*), the signal-to-noise ratio drops to 1 (Fig. 5, *h*), and the probability of an error in a bit increases to an unacceptable value of 10^{-2} (Fig. 5, *i*).

A decrease in the TD interval to 5 min raises the minimum of the RP towards the spacecraft to a level of 0.94 (Fig. 5, *j*) with an acceptable signal-to-noise ratio (Fig. 5, *k*) and the probability of an error in a bit (Fig. 5, *l*) by dynamic section.

An increase in the delay update interval to 1 min at the same minimum of the RP towards the spacecraft maintains the signal-to-noise ratio (Fig. 5, *m*) and the probability of a bit error (Fig. 5, *n*) at an acceptable level.

However, leveling the delay update interval to the level of the TD interval of 5 min lowers the minimum signal-to-noise ratio to 1 (Fig. 5, *o*), and raises the bit error probability to unacceptable 10-1 (Fig. 5, p).

A compromise combination of the duration of the TD interval dT_{TD} 2 min and the update interval of delays dT_{ud} = 1 min is shown in Fig. 6, *a* with a minimum of the RP towards the spacecraft of 0.9985 and acceptable deterioration of the signal-to-noise ratio (Fig. 6, *b*) and the probability of a bit error (Fig. 6, *c*). In general, Fig. 6 demonstrates a decrease in the quality of tracking with a decrease in the clock frequency of the offset F_s from 2 GHz (Fig. 6, *a – c*) to 500 MHz (Fig. 6, *d, e*) and 125 MHz (Fig. 6, *f, g*) with a fixed intermediate frequency F_{if} = 70 MHz, which suggests that the clock frequency of the shift F_s should be tied to the intermediate frequency F_{if}, at which, in fact, sampling and addition of the antenna signals are performed.

Figure 7 shows the results of a proportional decrease in the clock frequency of the shift F_s and the intermediate frequency F_{if} at the corresponding optimal values of the sampling frequency F_d and the sampling order m_d: F_{ai} = 70 MHz, F_d = 1.2903 MHz, m_d = 108, Fs = 2 GHz (Fig. 7, *a, b*); F_{if} = 17.5 MHz, F_d = 1.3208 MHz, m_d = 26; F_s = 500 MHz (Fig. 7, *c, d*); F_{if} = 2.1875 MHz, F_d = 1.75 MHz; m_d = 2, F_s = 62.5 MHz (Fig. 7, e, f). Analysis of the graphs in Fig. 7 shows that the hypothesis about the advisability of choosing the clock shift frequency F_s in proportion

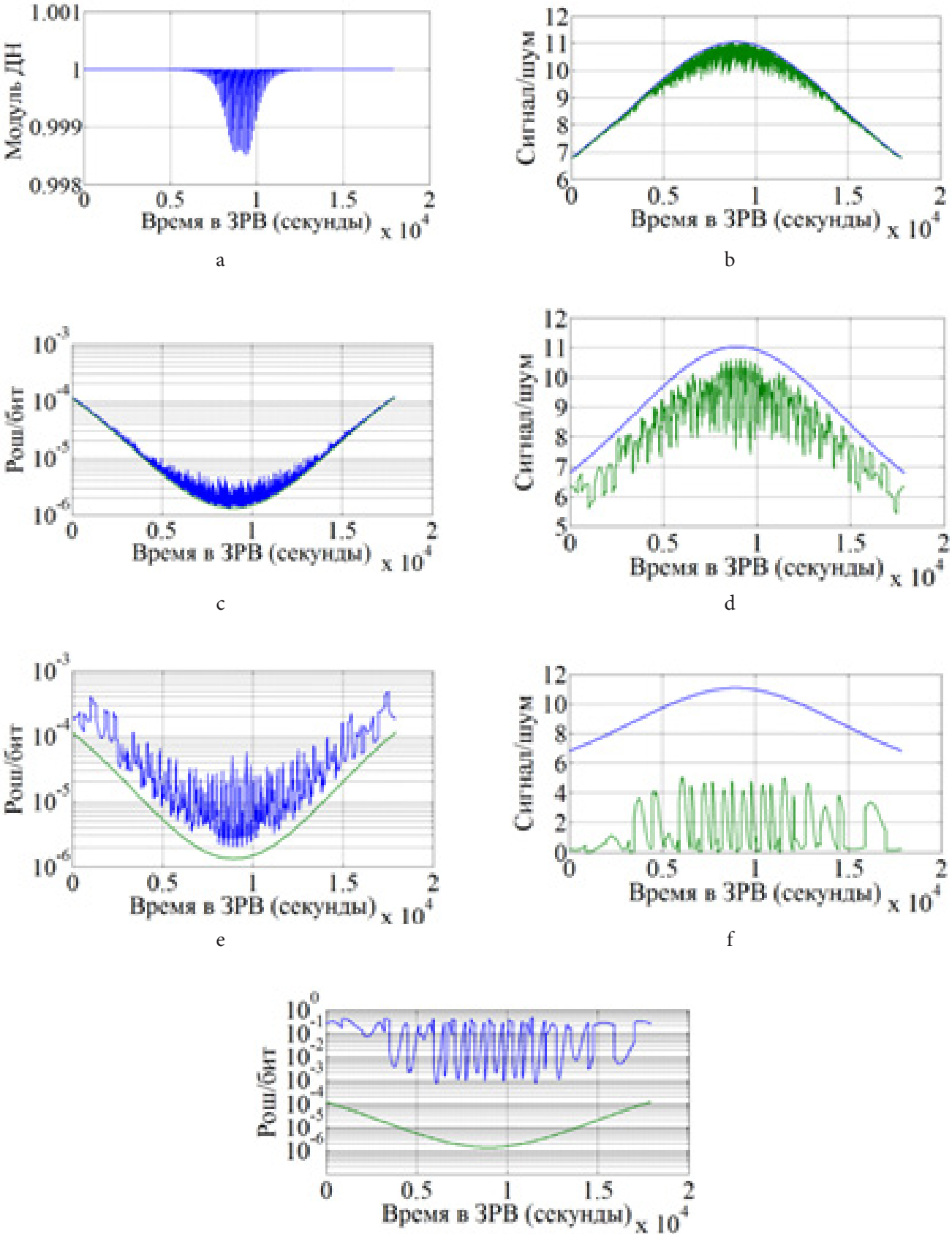

Fig. 6. Reduction of the clock frequency of the offset F_s from 2 GHz to 125 MHz with a fixed intermediate frequency F_{if} = 70 MHz

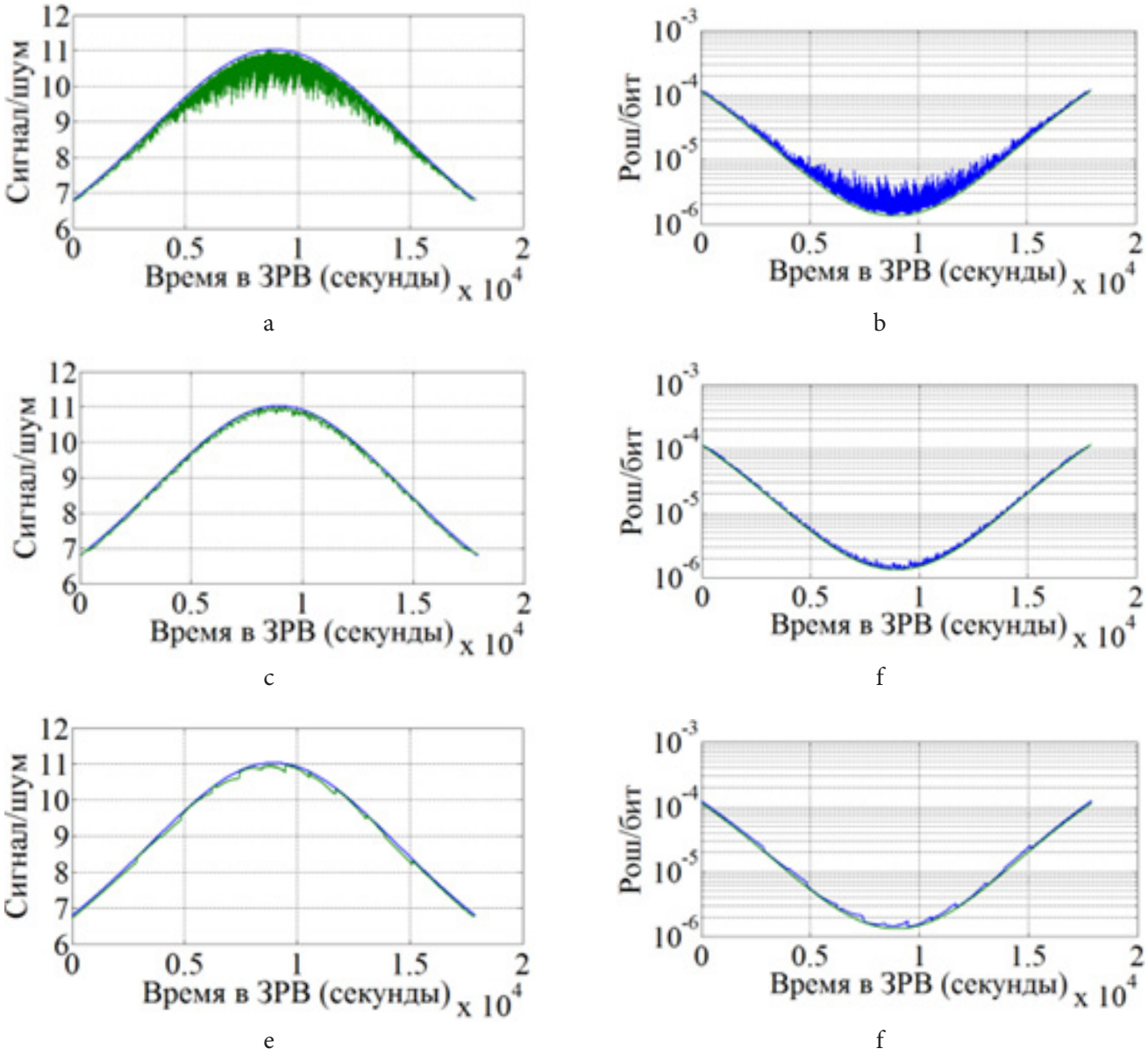

Fig. 7. Proportional reduction of the clock frequency of the shift F_s and intermediate frequency F_{if}

to the intermediate frequency F_{if} is correct: when the intermediate frequency F_{if} decreases to the permissible limit, when the sampling order m_d, determined by (39), remains greater than one, and the sampling frequency F_d, determined by (38), remains less than the intermediate frequency F_{if}, the variance of parameters is significantly reduced, and the graphs of the signal-to-noise ratio and the probability of a bit error fall closer to the theoretical limit.

The expediency of proportionality of the clock frequency of the shift F_s and the intermediate frequency F_{if} follows from the requirements of coherence (b) of the added antenna signals $\Delta T_s \cdot \Delta f << 1$ and the narrowband radio signal $\Delta f/F_{if} << 1$. Let $\Delta T_s \cdot \Delta f = d_k << 1$ and $\Delta f/F_{if} = d_y << 1$. Then $(\Delta f/F_{if})/(\Delta T_s \cdot \Delta f) = F_s/F_{if} = d_y/d_k = \text{const}$, QED. The simulation showed that the clock frequency of the shift F_s should be more than the intermediate frequency F_{if} by about $2000/70 \approx 30$ times. The coherence requirement is stricter by the same amount than the narrowband requirement.

Analysis of the graphs in Fig. 7 shows that an excessive increase in the intermediate frequency while maintaining the update interval of the delays leads to an increase in the spread of characteristics in the most dynamic section of the RVZ. This is due to the fact that during the update period, some error t_{er} accumulates in the delays, which

leads to a phase error of the corresponding signal $2\cdot\pi\cdot F_{if}\cdot t_{er}$. For small phase errors, sin (x) = x, that is, the amplitude error will be directly proportional to F_{if}. Therefore, when adding antenna signals with a shift in sampling pulses, it is advisable to choose an intermediate frequency as low as possible, however, just as when using VLBI methods.

Since the clock frequency of the shift F_s for the proposed method of combining the antenna signals is equivalent to the sampling frequency of the signals F_d in the VLBI method, the maximum speed of modern ADCs at the level of 1500 MHz [19] imposes restrictions on the use of VLBI methods at intermediate frequencies up to F_d / 30 = 1500/30 = 50 MHz. Proceeding from the fact that the sampling order cannot be less than m_d = 2, in accordance with (39) for the VLBI method, we obtain an estimate of the admissible upper frequency of the signal spectrum $F_w = F_{if}/(2m_d + 1) = 50/5 = 10$ MHz and the achievable speed transmission of information of the order of $F_w / m_{ls} = 10 / 1.25 = 8$ Mbit/s. The investigated method of adding radio signals with a shift of sampling pulses is implemented on pulse counters consisting of triggers, the maximum achievable clock frequency of which is currently about 10,000 MHz [20]. This corresponds to a maximum intermediate frequency of 10000/30 ≈ 300 MHz, a simple enough realizable sampling frequency $F_d = 4F_{if}/(2m_d + 1) = 300 \cdot 4/5=240$ MHz, allowable in the upper spectrum of the signal $F_d = F_{if}/(2m_d + 1) = 300/5 = 60$ MHz and an achievable information transfer rate of the order of $F_w/m_{ls} = 60 / 1.25 = 48$ Mbit / s.

Thus, the investigated method of combining the radio signals of the antennas of the antenna field with a shift of sampling pulses is potentially able to provide a six times higher rate of telemetry information transmission from deep space satellites in comparison with the classical VLBI method. However, it should be taken into account that this study was carried out on an idealized model of the process of tracking a spacecraft with an antenna field for target designations. Idealization consists in the fact that it is impossible to instantly change the angular velocity of the antenna movement due to inertia, therefore, at the nodal points, it is possible to achieve exact coincidence of either the angles or angular velocities of the antenna movement with the spacecraft movement. Therefore, in the future, it is planned to continue researching the proposed method, taking into account the inertia of the antennas.

References

1. Urlichich Yu.M., Gusev L.I., Leonov M.S. et al. *Radiotekhnicheskiye kompleksy dlya upravleniya dal'nimi kosmicheskimi apparatami i dlya nauchnykh issledovaniy* [Radio-technical complexes for controlling of deep-space spacecraft and for scientific research]. Ed. E.P. Molotov. Moscow, Fizmatlit, 2007, 232 p. (in Russian)
2. Molotov I.E. *Radiointerferometriya so svekhbol'shimi bazami (RSDB) – istoriya, sostoyaniye i apparatura* [Very large baseline interferometry (VLBI): history, state and equipment]. Electronic text. Available at: http://lfvn.astronomer.ru/report/0000007/p000007.htm (accessed 16 July 2020). (in Russian)
3. Slyusar V.I. Tsifrovye antennye reshetki v mobil'noy sputnikovoy svyazi [Digital antenna arrays in mobile satellite communication]. *Pervaya milya* [First mile], 2008, No. 4, pp. 10–15. (in Russian)
4. Voloshchuk I.V., Korolev N.A., Nikitin N.M. et al. Razvitie radiolokatsionnykh sredstv boevykh korabley na osnove tekhnologii tsifrovykh antennykh reshetok [Development of radiolocating facilities of combat vessels based on the technology of digital antenna arrays]. *Zbirnik naukovikh prats' Sevastopol'skogo viys'kovo-mors'kogo ordena Chervonoï Zirki institutu im. P.S.Nakhimova* [Proceedings of Admiral Nakhimov Naval Academy (Sevastopol)]. Sevastopol, SVMI im. P.S. Nakhimova, 2007, No. 2(12), 260 p.
5. Skolnik M. I. *Radar Handbook*. 3rd edition. The McGraw-Hill Book Companies, 2008. 1351 p.
6. Slyusar V.I. Tsifrovye antennye reshetki – budushchee radiolokatsii [Digital antennas arrays: Future of radiolocating]. *ELEKTRONIKA:* Nauka, Tekhnologiya, Biznes [ELECTRONICS: Science, Technology, Business], 2001, No. 3, pp. 42–46. (in Russian)
7. Slyusar V.I. SMART-antenny poshli v seriyu [SMART-antennas have come into serial production]. *Elektronika: Nauka, Tekhnologiya, Biznes* [Electronics: Science, Technology, Business], No. 2, 2004, pp. 62–65. (in Russian).
8. The Path to 4G Mobile. Communications Week International, Issue 260, 5 March 2001.

9. Slyusar V.I. Tsifrovye antennye reshetki resheniya zadach GPS [Digital antenna arrays to solve GPS tasks]. *Elektronika: Nauka, Tekhnologiya, Biznes* [Electronics: Science, Technology, Business], No. 1, 2009, pp. 74–78. (in Russian)
10. Backen S., Akos D.M. *Research Report "GNSS Antenna Arrays. Hardware requirements for algorithm implementation"*. Lulea University of Technology. Department of Computer Science and Electrical Engineering. April 4, 2006. Available at: http:// epubl.ltu.se/1402-1528/2006/13/LTU-FR-0613-SE.pdf.
11. Vatutin S.I., Zaytsev O.V. Primenenie mnogokanal'nykh tsifrovykh priemnykh ustroystv dlya sozdaniya antennykh poley NAKU KA [Using of multichannel digital receiving devices to create antenna fields of the ground-based automated control complex for spacecraft]. *Raketno-kosmicheskoe priborostroenie i informatsionnye tekhnologii* [Rocket-space device engineering and information systems]. 2013. *VI Vserossiyskaya nauchno-tekhnicheskaya konferentsiya "Aktual'nye problemy raketno-kosmicheskogo priborostroeniya i informatsionnykh tekhnologiy"* [Proceedings of the VI All-Russian scientific and technical conference "Current problems of rocket-space device engineering and information systems] (5–7 June 2013). Moscow, 2014, pp. 103–120. (in Russian)
12. Vatutin S.I., Zaytsev O.V. *Sposob obrabotki shirokopolosnykh signalov i ustroystvo fazirovaniya antenn priyema shirokopolosnykh signalov, preimushchestvenno dlya antenn neekvidistantnoy reshetki* [Method for processing broadband signals and device for phasing the antennas for receiving of broadband signals predominantly for the antennas of a non-uniform array]. Patent No. 2594385 of the Russian Federation. Patent holder: JSC "Russian Space Systems" (appl.: 25 May 2015, publ. 20 August 2016). (in Russian)
13. Vatutin S.I. Otsenka dopustimogo intervala vremeni obnovleniya zaderzhek rasprostraneniya signala mezhdu antennami tsifrovykh antennykh poley [Estimation of permissible time lag to update signal propagation delay between antennas of digital antenna fields]. *Raketno-kosmicheskoe priborostroenie i informatsionnye systemy* [Rocket and Space Device Engineering and Information Systems]. 2018, Vol. 5, No. 4, pp. 46–55. (in Russian).
14. Frolov O.P. *Antenny dlya zemnykh stantsiy sputnikovoy svyazi* [Antennas for ground stations of satellite communication]. Moscow, Radio i svyaz', 2000, 376 p. (in Russian)
15. Romanyuk Yu.A. Osnovy tsifrovoy obrabotki signalov [Fundamentals of digital signal processing]. In 3 parts. Part 1. *Svoystva i preobrazovaniya diskretnykh signalov: uchebnoye posobiye* [Properties and conversions of discrete signals: a tutorial]. Moscow, MFTI, 2005, 332 p. (in Russian)
16. Lyons R. *Tsifrovaya obrabotka signalov* [Understanding digital signal processing]. 2nd edition. Translated from English. Moscow, OOO "Binom-Press", 2006, 656 p. (in Russian)
17. Serkin F.B. Sravnitel'nyy analiz algoritmov otsenki otnosheniya signal-sh·chm na osnove kvadraturnykh komponent prinimayemogo signala [Analysis of signal-to-noise ratio estimation algorithms based on inphase and quadrature components of the received signal]. *Trudy MAI* (electronic journal). 2015. No. 83. Available at: http://www.mai.ru/upload/iblock/c80/serkin_vazhenin_veitsel_rus.pdf (accessed 16 July 2020). (in Russian)
18. Kotel'nikov V.A. *Teoriya potentsial'noy pomekhoustoychivosti* [Potential immunity theory]. Moscow–Leningrad: GEI, 1956, 152 p. (in Russian)
19. Shtraperin G.L. Bystrodeystvuyushchiye analogo-tsifrovyye preobrazovateli firmy National Semiconductor [High-speed analog-to-digital converters from National Semiconductor]. *Komponenty i tekhnologii* [Components and technologies], 2005, No.6, pp. 106–109. (in Russian)
20. NBSG53A 2.5V/3.3V SiGe selectable differential clock and data D flip-flop/clock divider with reset and OLS. Electronic text. Semiconductor Components Industries, LLC, 2008. September, 2008 – Rev. 13. Publication Order Number: NBSG53A/D. ON Semiconductor. Available at: http://onsemi.com.